

INNOVATIVE CHEMICALLY MODIFIED BIOSORBENT FOR REMOVAL OF PROCION RED

Fatin Izzaidah Anuar¹, Tony Hadibarata², Muryanto³, Adhi Yuniarto⁴,
Didik Priyandoko⁵, Ajeng Arum Sari^{3*}

¹Department of Environmental Engineering, Faculty of Civil Engineering, Universiti Teknologi Malaysia, 81310 UTM Skudai, Johor, Malaysia

²Department of Environmental Engineering, Faculty of Engineering and Science, Curtin University, CDT 250, Miri, Sarawak, Malaysia

³Research Center for Chemistry, Indonesian Institute of Sciences, Kawasan Puspiptek Serpong, Tangerang Selatan, Banten 15314, Indonesia

⁴Department of Environmental Engineering, Faculty of Civil, Environmental and Geo Engineering, Institut Teknologi Sepuluh Nopember, Surabaya 60111, Indonesia

⁵Department of Biology, Universitas Pendidikan Indonesia, Jalan Setiabudi 229, Bandung 40154, Indonesia

(Received: September 2018 / Revised: February 2019 / Accepted: May 2019)

ABSTRACT

The potential biosorbent of stinky bean peel (*Parkia speciosa*) (SBP) was investigated for azo dye Procion Red Mx-5B removal due to their accessibility, economically feasible, easy pre-treatment, and non-toxic. This study aims to determine the effect of chemically modified of the SBP, that a massive agricultural waste in Sarawak, to enhance its ability during adsorption of dye. The biosorbent used was dried, ground, and sieved through 600 μm sieve to obtain a similar average size. Impregnation with some chemicals was performed by using ZnCl_2 , K_2CO_3 , H_2SO_4 and NaOH for 24 h. The Freundlich, Langmuir, and Temkin techniques were examined to calculate the isotherm data. The result showed that the sorption capacity of the SBP was improved by ZnCl_2 modification. The equilibrium data were fitted with the Freundlich model, while the kinetic study was fitted with the pseudo-second-order kinetic model. Further, it was concluded that dyes uptake by biosorbent was based mainly on the role of carboxyl and a hydroxyl group.

Keywords: Biosorption; Chemical modification; Procion red; Stinky bean peel

1. INTRODUCTION

Dyes have been progressively utilized as a part of the material in textile, leather, paper, rubber, plastics, cosmetic industries, commercial nourishment enterprises as well as pharmaceuticals since these commonly have complex aromatic bonds which are more stable and biodegradable (Gong et al., 2005; Mane et al., 2007). At present, there are more than a thousand colors are commercially manufactured by the industry, where 20% is produced in the textile industry, and 15% are released into the environment during synthesis, processing or application (Liao et al., 2013). The discharge of dye wastewaters into the environment without any treatment caused eutrophication, perturbations in aquatic life such as photosynthesis obstructed, and aesthetic unpleasant. Numerous dyes present in the industry is the azo class which extensively becomes

*Corresponding author's email ajeng.a.sari@lipi.go.id, Tel. +62-21-7560929, Fax. +62-21-7560549
Permalink/DOI: <https://dx.doi.org/10.14716/ijtech.v10i4.2398>

a significant pollutant in dye effluents (Pandey et al., 2007). Azo dyes have one or more nitrogen bonds ($-N=N-$), sulfonic or aromatic groups which some of them have a half-life greater than 2000 h under daylight and imperviousness to biodegradation which danger for the environment (Grimes et al., 1999).

Various techniques had been applied to eliminate organic contaminants in the environment, such as coagulation/flocculation, filtration, reverse osmosis, membranes, advanced oxidation processes, and microbial degradation (Rubin & Soto, 2009; Hadibarata et al., 2011; Hadibarata et al., 2013). However, those treatments exhibit high capital, high cost and much maintenance besides multipart procedures. Inversely, biosorption is proof to be a simple technique due to the low cost of operation and simple design.

Biosorption is an alternative biotechnological process for removing organic and inorganic pollutants using natural and non-toxic sorbent. Another primary benefit of biosorption is easy to use very cheap materials as sorbents such as agriculture waste (Haghseresht & Lu, 1998; Grimes et al., 1999; Hayashi et al., 2000; Gong et al., 2008; Han et al., 2010; Han et al., 2011; Lam et al., 2017; Olufemi & Eniodunmo, 2018). Because of their accessibility, economically feasible, easy pre-treatment, and non-toxic, agricultural waste as biosorbents is increasingly used in pollution treatment.

Many techniques were implemented to improve biosorbent capability such as modification of the chemical composition of biosorbents which significantly increased the sorption capacity (Wirasnita et al., 2014). Modifications on biosorption properties were studied due to development of contact surface of biosorbent, by improving its porosity and removal capability. Additionally, the target of modification was the active functional groups on the biosorbent surface, that playing an important role for binding contaminants (Demirbas, 2008).

In this study, the chemical modification of SBP as biosorbent to remove PR solution was examined. Various parameters such as contact time, initial PR concentration and biosorbent dosage were conducted in batch studies. Kinetic and equilibrium studies were also considered to study the dye uptake onto SBP.

2. METHODS

2.1. Preparation of Dye Solutions

Procion Red Mx-5B (40% purity) was laboratory grade procured from Sigma–Aldrich. The series of 100, 200, 400, 600 and 800 mg/L of PR standard solution was prepared from 1000 ppm of dye as a stock solution.

2.2. Preparation of the Biosorbent

The preparation of the sample and chemical modification was following the modified method from Wirasnita et al. (2014). The stinky bean peel (SBP) used during the study were collected from urban areas in Johor Bahru. After washing with distilled water, the SBP was cut into small pieces and dried under ambient atmosphere for 24 hrs before being dried in the oven at 105 °C. Then it was ground and sieved through 600 µm sieve. The dried SBP was impregnated with some chemicals such as $ZnCl_2$, K_2CO_3 , H_2SO_4 and NaOH solution at 110°C for 24 h. After the solution was decanted off, the impregnated-SBP was dried in the oven at 105°C. Further, it was carbonized by a furnace using nitrogen gas at 500°C for 1 h. The modified SBP was washed with distilled water after cooling.

2.3. Characterization of the Biosorbent Materials

The surface morphology of the raw SBP before and after biosorption with PR solution was examined by Scanning Electron Microscopy (SEM) (JEOL 6335F-SEM, Japan). The functional

groups were investigated using Fourier transform infrared spectroscopy (FTIR) (Spectrum one, Perkin Elmer, USA) in the range of spectrum between 4000 to 400 cm^{-1} .

2.4. Equilibrium Study, Isotherm and Kinetic Studies

The modified SBP (5 g) was added to each flask with 50 ml of PR solutions with various concentrations. The mixtures were then shaken using mechanical shaker at 150 rpm in room temperature ($\pm 27^\circ\text{C}$). The biosorption kinetics was investigated in the ranging time from 0 to 24 h. The effect of biosorbent (20-140 mg/L) loading on PR biosorption was investigated. The sample was filtrated Advantec filter paper and measured by the acquisition of the UV/Vis spectrophotometer (NANOCOLOR VIS, Macherey-Nagel, Germany) at the maximum wavelength of 538 nm. All experiments were conducted in duplicate. The amount of dye removal (%) and adsorption capacity q_e (mg/g), were calculated by:

$$\text{Color removal (\%)} = \frac{C_o - C_e}{C_o} \times 100 \quad (1)$$

$$\text{Adsorption capacity} = \frac{C_o - C_e}{X} \times V \quad (2)$$

where C_o is the initial concentration of PR (mg/L), C_e is the equilibrium concentration of PR (mg/L), V is the volume of PR solution (L), and X is the mass of adsorbent (g) used (Doğan et al., 2008).

Three basic mathematical models of adsorption were used to determine the sorption abilities of SBP before and after the modifications, i.e. Langmuir, Freundlich, and Temkin. Langmuir is an empirical model that involves the formation of an adsorbate monolayer and crucial part of determining the maximum capacity of adsorbent (Vijayaraghavan et al., 2006). This model implicated that adsorption occurs at various particular sites within the adsorbent which neglect all kind of interaction between adsorbed substance (Hoda et al., 2006). Its equation model is expressed as:

$$\text{Langmuir equation, } \frac{C_e}{q_e} = \frac{1}{K_L q_m} + \frac{C_e}{q_m} \quad (3)$$

where C_e (mg/L) is the equilibrium of PR concentration, q_e (mg/g) is the equilibrium of amount of PR adsorbed, q_m is the maximum adsorption capacity (mg/g), and K_L is the Langmuir constant (L/mg).

The second adsorption isotherm was the Freundlich model which is intensively applied in a complex surface energy system especially for highly interactive species of adsorbent and molecular sieve. Distribution of heat and affinities were occurred in multilayer adsorption over the different surface (Zeldovich, 1934). The Freundlich isotherm can be represented as:

$$\text{Freundlich equation, } \ln q_e = \ln K_F + \left(\frac{1}{n}\right) \ln C_e \quad (4)$$

where K is a Freundlich constant, n is the Freundlich exponent coefficient.

The third model is Temkin isotherm that contains an element that unequivocally considers the adsorbing species–adsorbent interactions. In this isotherm, the interactions of adsorbent and adsorbate result gradually decreasing the binding energies and the heat of adsorption of molecules in the layer. The isotherm Temkin constants, B (Jmol^{-1}) which related to heat of adsorption can be calculated from the slope of q_e versus $\ln C_e$; while equilibrium binding constant, A (L/g)

corresponding to the maximum binding energy can be determined from the intercept of the plotting graph (Temkin & Pyzhev, 1940). The Temkin isotherm can be represented as follows:

$$\text{Temkin equation, } q_e = B \ln A + B \ln C_e \quad (5)$$

3. RESULTS AND DISCUSSION

3.1. Characteristic of Biosorbents

The biosorption process can be evaluated by the behavior of the functional group presented on the surface of biosorbent using Fourier Transform Infrared Spectroscopy (FTIR). Typically, agricultural waste is consisted by a similar functional group that playing an essential role in binding pollutants, such as carboxyl, alcohols, phenol, aldehydes, ether, and ketones (Pagnanelli et al., 2003). The functional group and the equal infrared biosorption frequency of PR are reported in Table 1. The broadband around 3367 cm^{-1} indicated the presence of stretch vibration of hydroxyl groups bonded on the surface of SBP. The peak appeared at 2929 cm^{-1} represented the asymmetrical stretch vibration of $-\text{CH}_3$. The active band at 1620 cm^{-1} showed the possible involvement of carboxylic acid with intermolecular hydrogen bond (Han et al., 2010) from the stretch vibration of $\text{C}=\text{O}$ groups. The peak at 1445 cm^{-1} was attributed to the symmetric bending of $-\text{CH}_3$. The biosorption peaks observed around 1357 cm^{-1} indicated the asymmetrical bending vibration of $-\text{CH}_3$ and $-\text{CH}_2$. The height at 1230 cm^{-1} characterized Si-O stretching and bending which meant the presence of silica (Al-Qodah & Shawabkah, 2009). The near bond exhibited at 1035 cm^{-1} could be assigned to the bending vibration of $-\text{OH}$ and stretching vibration of $\text{C}-\text{O}-\text{C}$ (Han et al., 2011).

Table 1 FTIR spectral characteristics of SBP before and after biosorption

Frequency (cm^{-1})		Assignment
Before adsorption	After adsorption	
3367	-	Bonded O-H groups
-	3409	N-H groups
2929	2925	CH_3 stretching groups
1620	-	$\text{C}=\text{O}$ stretching
-	1671	$\text{N}=\text{N}$ stretching
1445	-	CH_3 bending symmetric
-	1449	$\text{C}=\text{C}$ aromatic
1357	-	CH_3, CH_2 bending asymmetric
-	1375, 1324	C-N groups
1230	-	Si-O groups
-	1104	S=O groups
1035	1031	O-H bending, $\text{C}-\text{O}-\text{C}$ groups

The FTIR spectrum of SBP after biosorption showed that most of the functional groups of PR have appeared after the biosorption process. The peak at 3409 and 2925 cm^{-1} was presented the stretch vibration of amine N-H and aromatic $\text{C}=\text{C}$, respectively. The bond near 1671 cm^{-1} attributed to azo compound $\text{N}=\text{N}$ stretching vibrations. The band of $\text{C}=\text{C}$ aromatic ring was represented by the peak of 1449 cm^{-1} . The biosorption band around 1375 and 1324 cm^{-1} characterized the obtainable of amine group C-N. The peak exhibited near 1104 cm^{-1} shows that the presented of sulfones group S=O. The FTIR spectrum was showed the specific peaks in the fingerprint region 613 cm^{-1} which belongs to the halogen group of Cl. This result was similar to the previous study that the presence of carboxyl and hydroxyl groups affords the adsorption of organic pollutants (Kusrini et al., 2018).

Scanning Electron Microscopy (SEM) photographs of SBP before and after dye biosorption is shown in Figure 1. The porous texture of raw SBP has appeared with various sizes on the biosorbent surface. However, after the biosorption, the structure of biosorbent was a significant change. The raw SBP appears to have a rough pore on the surface which partially covered by PR molecules.

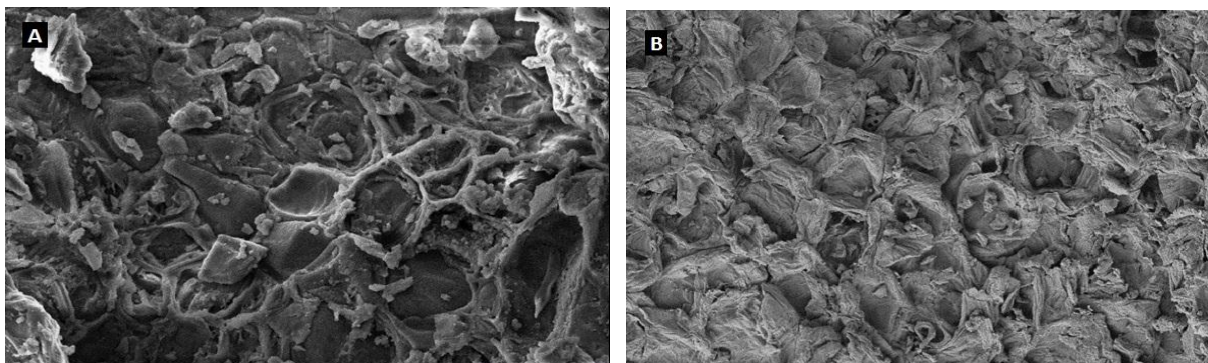


Figure 1 Morphology of structure raw sample of SBP (A); After biosorption of dye PR (B)

3.2. Chemical Modification

The first experiment was to specify equilibrium in the biosorption process. The effect of chemical modification on dye removal during the biosorption process was shown in Figure 2. Based on results, we assumed that the equilibrium state is achieved at 4 h. According to effect as shown in Figure 2, only chemical activation using $ZnCl_2$ gives the satisfied result to remove PR compared with K_2CO_3 , $NaOH$, and H_2SO_4 . It was assumed that only $ZnCl_2$ that can develop micropores and creates active sites on SBP, therefore biosorption of PR using $ZnCl_2$ SBP modification was chosen (Hayashi et al., 2000).

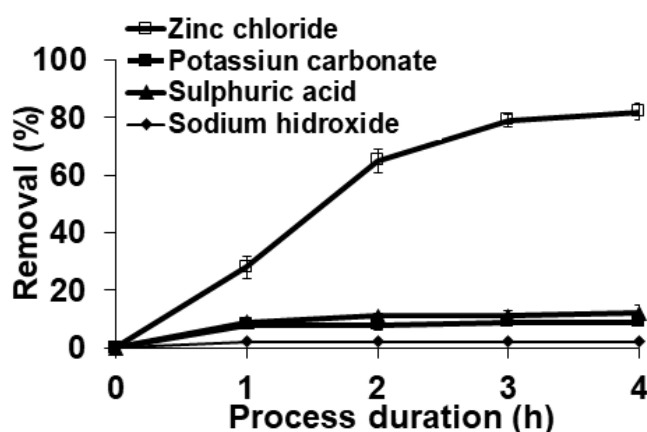


Figure 2 The effect of chemical modification on dye removal during the biosorption process

Chemicals such as H_3PO_4 , $ZnCl_2$, and KOH were commonly used to either weaken or break down the chemical bonds in the lignocellulosic components from biomass. Further, the formation of pores was increased, and these components were quickly transformed into volatiles (Lam et al., 2017). However, several optimizations of the parameters of activation, such as temperature, time, chemical precursor weight ratio are needed to obtain better effectiveness in removal of dye (Nowicki et al., 2016).

3.3. Effect of Contact Time, Initial Dye Concentration and Biosorbent Dosage

The effect of contact time on the biosorption of PR by SBP was explored to investigate the transfer phenomena during the biosorption process. The experiment was conducted with an initial concentration of 1000 mg/L with biosorbent dosage of 100 mg/L. In the first 3 h, rapid biosorption

of PR has occurred; after that, it was slower biosorption within the period of 12–24 h. The percentage PR removal of 77.43% was obtained during equilibrium in about 12 h with its biosorption capacity of 7.743 mg/g. The biosorption process was quickly raised within the first 3 h due to the availability of the readily accessible sites (Figure 3A). After 12 h, the biosorbent surface was fully occupied with PR and reduce the available sites thus reduce the biosorption process. Finally, the plateau was reached after 12 h indicated that biosorbent was saturated (Wirasnita et al., 2014). Furthermore, the biosorption phenomena of SBP take a relatively long contact time. For the most part, the PR molecules need first to experience the limit layer impact, then adsorb from the surface lastly diffuse into the porous structure of the biosorbent (Wong et al., 2009).

The effects of the initial concentration of PR have been studied from 50 to 1000 mg/L. Figure 3B indicated that the percentage removal of PR was decreased from 99.8 to 82.04% when the initial concentration increased. The biosorption capacity expanded from 0.499 to 8.204 mg/g when initial level increased. Increasing the initial level raised the driving force of mass transfer as well as increase the potential of interaction between the molecules of PR and SBP, thus, resulting in higher biosorption capacity (Tan et al., 2008).

The effect of biosorbent loading of SBP toward the biosorption of PR was evaluated by varying the amount of biosorbent concentration from 20 to 140 mg/L. Figure 3C indicated that increasing biosorbent dosage resulted in increasing the percentage removal of PR. The incremental of PR removal becomes very low at biosorbent concentration 100 mg/L, and the biosorbent surface tends to saturated at biosorbent concentration 120 mg/L. An increase the biosorbent dosage can attribute to a more significant surface area, and more biosorption sites were produced. The biosorption process becomes very low at biosorbent concentration 120 mg/L due to the PR solution come to equilibrium (Mane et al., 2007). However, increasing the biosorbent dosage caused decreasing the biosorption capacity of the biosorbent.

The maximum removal of PR was at biosorbent loading of 100 and 120 mg/L. Additional of biosorbent concentration was not reflected the change of removal. Nevertheless, the biosorption capacity for the loading of 120 g/L was 7.52 mg/g. It was less than biosorbent loading 100 g/L that was 8.2 mg/g. Thus the effective biosorbent dosage for removal of PR from 50 mL aliquot of 1000 mg/L was 100 mg/L. A similar trend had been reported by previous studies (Ghaedi et al., 2013; Senthil Kumar et al., 2010).

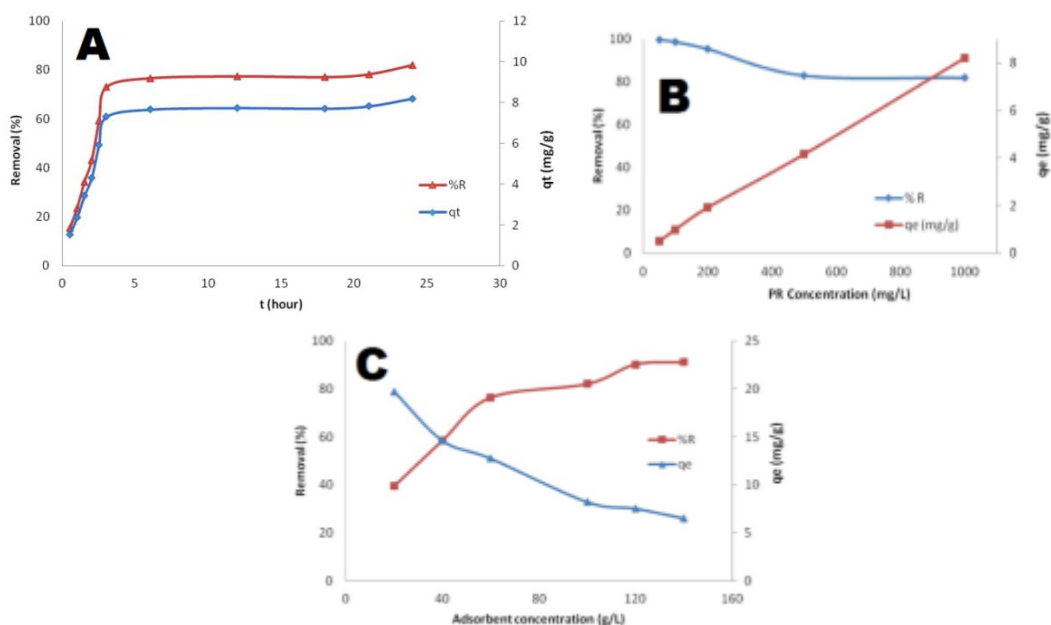


Figure 3 (A) Effect of contact time on PR biosorption ($C_0 = 1000\text{mg/L}$; adsorbent conc. = 100 mg/L); (B) Effect of initial PR concentration on biosorption (adsorbent conc. = 100 mg/L, time = 24 hrs); (C) Effect of biosorbent dosage on PR adsorption ($C_0 = 1000\text{ mg/L}$, time = 24hrs)

3.4. Isotherm and Kinetic Studies

Biosorption isotherm of PR has been observed by varying the amount of biosorbent dosage (1, 3 and 5 g). The plot of C_e/q_e versus C_e in Figure 4A indicated the biosorption of PR by SBP performed a weak correlation coefficient (R^2) for Langmuir isotherm with $R^2 = 0.6938$, 0.6904 and 0.8433 for biosorbent dosage 1, 3 and 5 g, respectively. The values of q_m can be obtained from the slope while K_L calculated from the intercept of the linear plot which is showed in Table 2. In general, K_F value increases when biosorption capacity of biosorbent increases. The amount of $1/n$ indicated the favorability of biosorption. It has represented the measure of biosorption intensity of surface heterogeneity. Typically, the values of $n > 1$ more favorable biosorption condition (Treybal, 1968) and $1/n$ closer to zero specified the more heterogeneous biosorption (Haghseresht & Lu, 1998). The linear plot in Figure 4 shows that biosorption of PR by SBP has an excellent fitting curve for Freundlich isotherm with the correlation coefficient $R^2 = 0.9993$, 0.9786 and 0.9728 for 1, 3 and 5 g of biosorbent dosage. The values of K_F and n can be calculated from the intercept and the slope of the graph as stated in Table 2.

Table 2 The adsorption isotherm parameters of PR biosorption

Adsorbent amount (g)	Langmuir			Freundlich				Temkin		
	q_m	K_L	R^2	n	K_F	q_m	R^2	A	B	R^2
1	27.3157	0.0028	0.6938	1.6681	0.3469	21.8101	0.9993	0.0640	4.1873	0.7869
3	15.3619	0.0077	0.6904	1.6801	0.3556	21.7055	0.9786	0.2181	2.2714	0.7714
5	8.0451	0.0433	0.8433	2.7959	0.9937	11.7558	0.9728	4.8928	0.8889	0.7482

Linear plot of q_e versus $\ln C_e$ for the sample of PR Figure 4 shows that biosorption does not follow the Temkin model which correlation coefficient $R^2 = 0.7869$, 0.7714 and 0.7482 for biosorbent dosage 1, 3 and 5 g, respectively. Hence, by comparing the correlation factor, Freundlich isotherm was the best model to represent the biosorption of PR by SBP. The result suggested that the biosorption is favorable with values of $n > 1$ for all biosorbent amount. The intensity value increased in the high amount of biosorbent dosage indicated the biosorption process was more favorable with $n = 1.67$, 1.68 and 2.80 for 1, 3 and 5 g, respectively. Table 3 specified the K_F , n , and Q_{max} value of SBP in our study compared with other biosorbent to adsorb dyes.

Table 3 Freundlich Isotherm for biosorption of dyes by various biosorbent

Dye	Biosorbent	K_F	n	Q_m	References
Basic dye	Granular activated carbon	77.82	8.121	149.429	Meshko et al., 2001
Basic dye	Natural zeolite	2.574	3.256	13.101	Meshko et al., 2001
Acid Red 57	Acid activated bentonite	3.18	1.27	732.204	Özcan & Özcan, 2004
Dye BB3	Sugarcane bagasse	0.14	0.74	122.121	Wong et al., 2009
Congo Red	Coir pith activated carbon	2.53	3.39	6.122	Namasivayam & Kavitha, 2002
Dye wastewater	Mahogany sawdust	88.3	3.98	500.875	Malik, 2004
Procion Red	Stinky Bean Peel	0.994	2.8	11.759	This study

The PR sorption kinetic was investigated by determining the effect of contact time on the removal of PR for 24 h. The significant to evaluate the reaction kinetics is to understand the dynamics of

biosorbents uptake during the process in term of the order of rate constant. Therefore, to assess the biosorption of PR onto SBP, Pseudo-first-order, Pseudo-second-order and intraparticle diffusion kinetic models were used like the following equations:

$$\text{Pseudo-first-order, } \ln(q_e - q_t) = \ln q_e - k_1 t \tag{6}$$

$$\text{Pseudo-second-order, } \frac{t}{q_t} = \frac{1}{k_2 q_e^2} + \frac{t}{q_e} \tag{7}$$

$$\text{Intraparticle diffusion, } qt = k_{diff} t^{1/2} + C \tag{8}$$

where q_e is the amount of PR adsorbed at equilibrium (mg/g), q_t is the amount of PR adsorbed at time t (min), k_1 is the rate constant of pseudo-first-order, k_2 is the rate constant of pseudo-second-order, k_{dif} is the intraparticle diffusion rate constant (mg/g min^{1/2}), C is the intercept which indicates the boundary layer thickness. The larger the intercept is the greatest boundary layer effect.

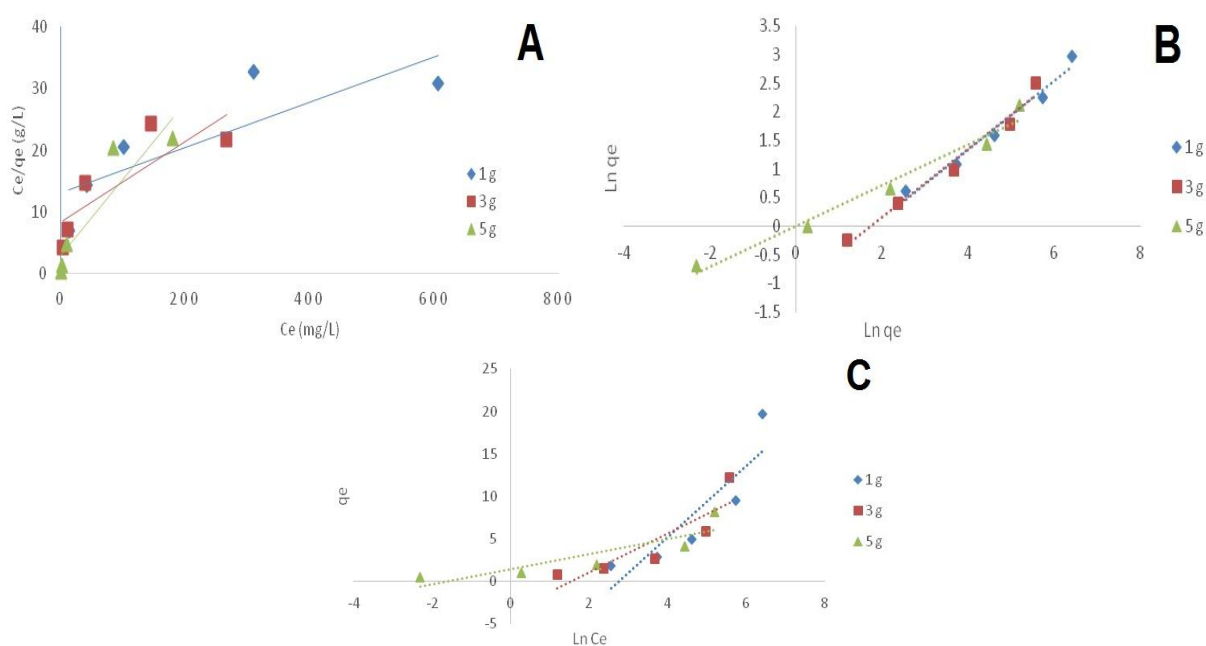


Figure 4 Langmuir isotherm model (A), Freundlich isotherm model (B), Temkin isotherm model (C) for the biosorption of PR by SBP

The value of the rate constant (k_1) for the biosorption of PR by SBP can be obtained from the slope of $\ln(q_e - q_t)$ against t while rate constant (k_2) can be calculated from the plot of t/q_t versus t and k_{dif} can be determined from q_t versus $t^{1/2}$. Table 4 represented the kinetics parameters for the experimental data that the pseudo-second-order model described the best fit which the correlation coefficient was 0.995 compared to the pseudo-first-order model where the correlation coefficient was 0.659.

Table 4 Kinetic parameter of PR biosorption

Kinetic model	Parameter	Kinetic model	Parameter	Kinetic model	Parameter
q_e experiment (mg/g)	8.2040				
<i>Pseudo-first-order</i>		<i>Pseudo-second-order</i>		<i>Interparticle- diffusion</i>	
q_e calculated (mg/g)	1.8123	q_e calculated (mg/g)	8.6881	I	3.7544
K_f	0.0007	K_s	0.0010	k_{id}	0.0064
R^2	0.6587	R^2	0.9950	R^2	0.5796

Furthermore, the value of experimental q_e ($q_{e,exp}$) was much closer to the calculated value of q_e ($q_{e,cal}$) which were 8.204 (mg/g) and 8.69 (mg/g) respectively for the pseudo-second-order model. The biosorption process was controlled by the particle diffusion if the good fitting curve performed by the plot of q_t versus $t^{1/2}$. Table 4 indicated the poor correlation coefficient (0.5796) for the diffusion mechanism of PR into SBP. The result gives an idea the diffusion process does not contribute to intra-particle diffusion.

Kinetic modelling through the pseudo-second-order model indicated that the adsorption of dye onto biosorbent came from a chemisorption process that supported by the presence of metals in the solution (Azzaz et al., 2017).

4. CONCLUSION

The present study proved that the raw SBP was potential to be used as biosorbent to remove PR from aqueous solution. The biosorption time was 12 h with 77.43% removal. Based on FT-IR analysis, the presence of carboxyl and hydroxyl groups affords the adsorption of organic pollutants. The biosorption follows the pseudo-second-order of kinetic model with R^2 of 0.995. The isotherm data indicated that Freundlich isotherm showed better correlation coefficient with $R^2 = 0.9993, 0.9786$ and 0.9728 for 1, 3 and 5 g of biosorbent dosage. This biosorbent is valuable since they are green, economical, and easy to prepare with a simple design of biosorption technique

5. ACKNOWLEDGEMENT

A part of this research was financially supported by a Fundamental Research Grant Scheme (FRGS) of Ministry of High Education Malaysia (No. 4F465).

6. REFERENCES

- Al-Qodah, Z., Shawabkha, R., 2009. Production and Characterization of Granular Activated Carbon from Activated Sludge. *Brazilian Journal of Chemical Engineering*, Volume 26(1), pp. 127–136
- Azzaz, A.A., Jellali, S., Akrouf, H., Assadi, A.A., Bousselmi, L., 2017. Optimization of a Cationic Dye Removal by a Chemically Modified Agriculture by-product using Response Surface Methodology: Biomasses Characterization and Adsorption Properties. *Environmental Science and Pollution Research*, Volume 24(11), pp. 9831–9846
- Demirbas, A., 2008. Heavy Metal Adsorption onto Agro-based Waste Materials: A Review. *Journal of Hazardous Materials*, Volume 157(2-3), pp. 220–229
- Doğan, M., Abak, H., Alkan, M., 2008. Biosorption of Methylene Blue from Aqueous Solutions by Hazelnut Shells: Equilibrium, Parameters and Isotherms. *Water, Air, and Soil Pollution*, Volume 192(1–4), pp. 141–153
- Ghaedi, M., Karimi, F., Barazesh, B., Sahraei, R., Daneshfar, A., 2013. Removal of Reactive Orange 12 from Aqueous Solutions by Adsorption on Tin Sulfide Nanoparticle Loaded on Activated Carbon. *Journal of Industrial and Engineering Chemistry*, Volume 19(3), pp. 756–763
- Gong, R., Sun, Y., Chen, J., Liu, H., Yang, C., 2005. Effect of Chemical Modification on Dye Adsorption Capacity of Peanut Hull. *Dyes and Pigments*, Volume 67(3), pp. 175–181
- Gong, R., Zhu, S., Zhang, D., Chen, J., Ni, S., Guan, R., 2008. Adsorption Behavior of Cationic Dyes on Citric Acid Esterifying Wheat Straw: Kinetic and Thermodynamic Profile. *Desalination*, Volume 230(1–3), pp. 220–228
- Grimes, D.I., Pardo-Igúzquiza, E., Bonifacio, R., 1999. Optimal Areal Rainfall Estimation using Raingauges and Satellite Data. *Journal of Hydrology*, Volume 222(1–4), pp. 93–108

- Haghseresht, F., Lu, G.Q., 1998. Adsorption Characteristics of Phenolic Compounds onto Coal-Reject-Derived Adsorbents. *Energy and Fuels*, Volume 12(6), pp. 1100–1107
- Han, R., Zhang, L., Song, C., Zhang, M., Zhu, H., Zhang, L., 2010. Characterization of Modified Wheat Straw, Kinetic and Equilibrium Study about Copper Ion and Methylene Blue Adsorption in Batch Mode. *Carbohydrate Polymers*, Volume 79(4), pp. 1140–1149
- Han, X., Wang, W., Ma, X., 2011. Adsorption Characteristics of Methylene Blue onto Low Cost Biomass Material Lotus Leaf. *Chemical Engineering Journal*, Volume 171(1), pp. 1–8
- Hadibarata, T., Tachibana, S., Askari, M., 2011. Identification of Metabolites from Phenanthrene Oxidation by Phenoloxidases and Dioxygenases of *Polyporus* sp. S133. *Journal of Microbiology and Biotechnology*, Volume 21(3), pp. 299–304
- Hadibarata, T., Chuang, T.Z., Rubiyatno, Zubir, M.M.F.A., Khudhair, A.B., Yusoff, A.R.M., Salim, M.R., Hidayat, T., 2013. Identification of Naphthalene Metabolism by White Rot Fungus *Pleurotus eryngii*. *Bioprocess and Biosystem Engineering*, Volume 36(10), pp. 1455–1461
- Hayashi, J., Kazehaya, A., Muroyama, K., Watkinson, A.P., 2000. Preparation of Activated Carbon from Lignin by Chemical Activation. *Carbon*, Volume 38(13), pp. 1873–1878
- Hoda, N., Bayram, E., Ayranci, E., 2006. Kinetic and Equilibrium Studies on the Removal of Acid Dyes from Aqueous Solutions by Adsorption onto Activated Carbon Cloth. *Journal of Hazardous Materials*, Volume 137(1), pp. 344–351
- Kusrini, E., Kinastiti, D.D., Wilson, L.D., Usman, A., Rahman, A., 2018. Adsorption of Lanthanide Ions from an Aqueous Solution in Multicomponent Systems using Activated Carbon from Banana Peels (*Musa paradisiaca* L.). *International Journal of Technology*, Volume 9(6), pp. 1132–1139
- Lam, S.S., Liew, R.K., Wong, Y.M., Yek, N.Y.P., Ma, N.L., Lee, C.L., Chase, H.A., 2017. Microwave-assisted Pyrolysis with Chemical Activation, an Innovative Method to Convert Orange Peel into Activated Carbon with Improved Properties as Dye Adsorbent. *Journal of Cleaner Production*, Volume 162, pp. 1376–1387
- Liao, C.-S., Hung, C.-H., Chao, S.-L., 2013. Decolorization of Azo Dye Reactive Black B by *Bacillus Cereus* Strain Hj-1. *Chemosphere*, Volume 90(7), pp. 2109–2114
- Malik, P.K., 2004. Dye Removal from Wastewater using Activated Carbon Developed from Sawdust: Adsorption Equilibrium and Kinetics. *Journal of Hazardous Materials*, Volume 113(1), pp. 81–88
- Mane, V.S., Deo Mall, I., Chandra Srivastava, V., 2007. Kinetic and Equilibrium Isotherm Studies for the Adsorptive Removal of Brilliant Green Dye from Aqueous Solution by Rice Husk Ash. *Journal of Environmental Management*, Volume 84(4), pp. 390–400
- Meshko, V., Markovska, L., Mincheva, M., Rodrigues, A.E., 2001. Adsorption of Basic Dye on Granular Activated Carbon and Natural Zeolite. *Water Research*, Volume 35(14), pp. 3357–3366
- Namasivayam, C., Kavitha, D., 2002. Removal of Congo Red from Water by Adsorption onto Activated Carbon Prepared from Coir Pith, an Agricultural Solid Waste. *Dyes and Pigments*, Volume 54(1), pp. 47–58
- Nowicki, P., Kazmierczak-Razna, J., Pietrzak, R., 2016. Physicochemical and Adsorption Properties of Carbonaceous Sorbents Prepared by Activation of Tropical Fruit Skins with Potassium Carbonate. *Materials & Design*, Volume 90, pp. 579–585
- Olufemi, B., Eniodunmo, O., 2018. Adsorption of Nickel(II) Ions from Aqueous Solution using Banana Peel and Coconut Shell. *International Journal of Technology*, Volume 9(3), pp. 434–445
- Özcan, A.S., Özcan, A., 2004. Adsorption of Acid Dyes from Aqueous Solutions onto Acid-Activated Bentonite. *Journal of Colloid and Interface*, Volume 276(1), pp. 39–46
- Pagnanelli, F., Mainelli, S., Vegliò, F., Toro, L., 2003. Heavy Metal Removal by Olive Pomace:

- Biosorbent Characterisation and Equilibrium Modelling. *Chemical Engineering Science*, Volume 58(20), pp. 4709–4717
- Pandey, A., Singh, P., Iyengar, L., 2007. Bacterial Decolorization and Degradation of Azo Dyes. *International Biodeterioration & Biodegradation*, Volume 59(2), pp. 73–84
- Rubin, B.S., Soto, A.M., 2009. Bisphenol A: Perinatal Exposure and Body Weight. *Molecular and Cellular Endocrinology*, Volume 304(1–2), pp. 55–62
- Senthil Kumar, P., Ramalingam, S., Senthamarai, C., Niranjanaa, M., Vijayalakshmi, P., Sivanesan, S., 2010. Adsorption of Dye from Aqueous Solution by Cashew Nut Shell: Studies on Equilibrium Isotherm, Kinetics and Thermodynamics of Interactions. *Desalination*, Volume 261(1–2), pp. 52–60
- Tan, I.A.W., Ahmad, A.L., Hameed, B.H., 2008. Adsorption of Basic Dye on High-Surface-Area Activated Carbon Prepared from Coconut Husk: Equilibrium, Kinetic and Thermodynamic Studies. *Journal of Hazardous Materials*, Volume 154(1–3), pp. 337–346
- Temkin, M.J., Pyzhev, V., 1940. Kinetics of Ammonia Synthesis on Promoted Iron Catalysts. *Acta Physicochimica URSS*, Volume 12, pp. 217–222
- Treybal, R.E., 1968. *Mass-Transfer Operations*. 3rd ed. McGraw-Hill, New York
- Vijayaraghavan, K., Padmesh, T.V.N., Palanivelu, K., Velan, M., 2006. Biosorption of Nickel (II) Ions onto *Sargassum Wightii*: Application of Two-Parameter and Three-Parameter Isotherm Models. *Journal of Hazardous Materials*, Volume 133(1–3), pp. 304–308
- Wirasnita, R., Hadibarata, T., Yusoff, A.R.M., Yusop, Z., 2014. Removal of Bisphenol A from Aqueous Solution by Activated Carbon Derived from Oil Palm Empty Fruit Bunch. *Water, Air, & Soil Pollution*, Volume 225(2148), pp. 1–12
- Wong, S.Y., Tan, Y.P., Abdullah, A.H., Ong, S.T., 2009. The Removal of Basic and Reactive Dyes using Quartenised Sugar Cane Bagasse. *Journal of Physical Therapy Science*, Volume 20(1), pp. 59–74
- Zeldovich, J.B., 1934. Adsorption Site Energy Distribution. *Acta physicochimica URSS*, Volume 1, pp. 961–973